



**Achiral straight-rod liquid crystals indicating local biaxiality  
and ferroelectric switching behavior in the smectic A and  
nematic phases**

Journal:	<i>Journal of Materials Chemistry C</i>
Manuscript ID:	TC-ART-02-2015-000389.R1
Article Type:	Paper
Date Submitted by the Author:	28-Feb-2015
Complete List of Authors:	Kishikawa, Keiki; Chiba University, Faculty of Engineering Inoue, Takahiro; Chiba University, Hasegawa, Naoshi; Chiba University, Takahashi, Masahiro; Chiba University, Kohri, Michinari; Chiba university, Taniguchi, Tatsuo; Chiba University, Kohmoto, Shigeo; Chiba University,

## ARTICLE

# Achiral straight-rod liquid crystals indicating local biaxiality and ferroelectric switching behavior in the smectic A and nematic phases

Cite this: DOI: 10.1039/x0xx00000x

Received 00th January 2012,  
Accepted 00th January 2012

DOI: 10.1039/x0xx00000x

[www.rsc.org/](http://www.rsc.org/)

Keiki Kishikawa\* Takahiro Inoue, Naoshi Hasegawa, Masahiro Takahashi, Michinari Kohri, Tatsuo Taniguchi and Shigeo Kohmoto

Biaxial smectic A ( $SmA_b$ ) and biaxial nematic ( $N_b$ ) liquid crystal (LC) phases using achiral straight-rod molecules were realized through perfluoroarene-arene (PFA-A) and CH/F interactions. Compounds **1a**, **1b** and **1c**, 4,4'-(2,3,4-trifluorobenzoyloxy)biphenyl, 4,4'-(2,3-difluorobenzoyloxy)biphenyl and 4,4'-(2-fluorobenzoyloxy)biphenyl were synthesized. The liquid crystallinity of these compounds was investigated using polarized light optical microscopy (POM) and differential scanning calorimetry (DSC). Furthermore, the ferroelectric switching behaviors of **1a** in the nematic ( $N$ ) and smectic A ( $SmA$ ) LC phases and **1b** in the  $N$  phase were confirmed by applying a triangular wave voltage in electro-optic experiments. Then, the values of spontaneous polarization ( $P_s$ ) in the LC phases of **1a** were investigated as functions of frequency, voltage, and temperature. It was strongly hypothesized that the semiperfluorinated phenyl (SFP) groups rotate around the molecular long axes and change pairs in the CH/F interacting sites, and this cooperative movement of the SFP groups is repeated during the switching process.

## Introduction

$N_b$  and  $SmA_b$  LC phases, which have a lateral order in addition to the directional order along the long molecular axis, are expected to be a strong candidate for next-generation LC displays (LCDs) because of their fast response.<sup>1,2</sup> On the one hand, in present LCD devices, rod-like molecules in a uniaxial nematic ( $N_u$ ) phase that possesses one-directional order change the directions of their molecular long axes by switching an electric field-on and -off. On the other hand, in  $N_b$  or  $SmA_b$  phases, each molecule only changes the direction of its short axis around the molecular long axis during the light-switching process.<sup>1-3</sup> It has been reported that the difference in the molecular movements between the  $N_b$  (or  $SmA_b$ ) and  $N_u$  (or uniaxial  $SmA$ ) phases results in a large difference in their electro-responsiveness because the biaxial and uniaxial phases have significantly different excluded volumes during switching process.<sup>1,2,4</sup>

To realize biaxiality in  $N$  and  $SmA$  phases, molecules with an anisotropic shape (bent rod<sup>5-11</sup> and board<sup>12</sup>) or covalently linked mesogens (LC molecules consisting of disc and rod units,<sup>13</sup> bent rod-shaped LC dimers<sup>14-16</sup> and LC polymers<sup>17</sup>) have been used. It is also known that a mixture of rod-like and bent-core molecules are effective to generate biaxiality in  $N$  and  $SmA$

phases.<sup>18</sup> However, an increase in the anisotropy is a tradeoff between stable biaxiality and high responsiveness because of the increase in the excluded volume during the switching process. In this paper, we describe the realization of  $N_b$  and  $SmA_b$  phases of simple rod-like molecules and their ferroelectric switching behaviors. A few examples of ferroelectric switching behaviors have been reported only in bent-core liquid crystalline compounds, and a bent rod shape is thought to be essential for ferroelectric switching.<sup>19,20</sup> To the best of our knowledge, this is the first example of  $N_b$  and  $SmA_b$  phases of achiral rod-like molecules that exhibit ferroelectric switching.

To realize ferroelectrically switchable  $N_b$  and  $SmA_b$  phases of achiral rod-like molecules, we designed novel rod-like molecules based on an interaction-assisted approach. Namely, our molecules possess 1) strong intermolecular face-to-face and edge-to-edge interactions, and 2) a large lateral molecular dipole. As shown in Fig. 1, introducing strong face-to-face and edge-to-edge interactions changes a uniaxial mesophase (A) into a biaxial mesophase (B).<sup>21-23</sup> If each rod-like molecule in the biaxial mesophase has a lateral molecular dipole, the directions of the molecular short axes can be switched by applying an electric field (C).

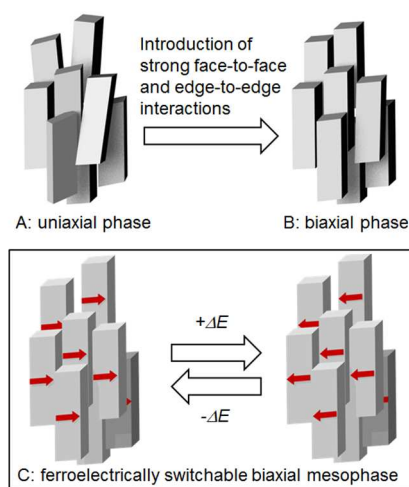


**Fig. 1** Concept for changing a uniaxial mesophase (A) to a biaxial mesophase (B) by introducing strong face-to-face and edge-to-edge interactions in rod-like molecules, and the realization of a ferroelectrically switchable biaxial mesophase (C) by introducing a lateral molecular dipole (red arrow) into each molecule (C).

In this molecular design, perfluoroarene-arene (PFA-A)<sup>24-26</sup> and C-H/F<sup>27</sup> interactions were selected as the face-to-face and edge-to-edge interactions, respectively. The PFA-A interaction is known as the face-to-face interaction between perfluorinated and non-fluorinated arenes which consists of van der Waals and Coulomb forces.<sup>28</sup> For example, the interaction between hexafluorobenzene and benzene molecules has been estimated to be 3.7-5.6 kcal/mol.<sup>29-30</sup> On the other hand, the C-H/F interaction primarily consists of the Coulomb force between hydrogen and fluorine atoms, and the value between one fluorine atom and one hydrogen atom has been estimated to be approximately 0.4-1.0 kcal/mol.<sup>31</sup>

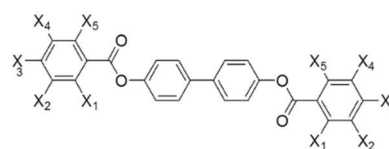
These interaction sites are concentrated in our achiral rod-like molecules **1a-c**, 4,4'-(2,3,4-trifluorobenzoyloxy)biphenyl, 4,4'-(2,3-difluorobenzoyloxy)biphenyl and 4,4'-(2-fluorobenzoyloxy)biphenyl as shown in Fig. 2. In these molecules, two semiperfluorinated phenyl (SFP) moieties (tri-, di-, or mono-fluorinated benzoyloxy groups) are introduced at both terminals of the biphenyl moiety. We hypothesized that semiperfluorinated arene-arene (SFA-A) and C-H/F interactions would interact between these molecules in a LC state to generate  $N_b$  or  $SmA_b$  phases and that the molecules would respond cooperatively as a ferroelectric phase to an applied electric field. Alkyl chains were not introduced in these molecules to avoid weakening the intermolecular interactions, which also simplified the molecular structures. The simplicity of their molecular structures would be useful for estimating the molecular motions in this switching system.

## Results and Discussion

### Phase identification of the LC compounds using POM and DSC

Compounds **1a-c** were synthesized via the condensation of 4,4'-biphenol and the corresponding semiperfluorinated benzoic acid. Their phase transition behaviors are shown in Fig. 2. The phases were identified using polarized light optical

microscopy (POM). The microphotographs are shown in Fig. 3. Compound **1a** exhibited stable  $SmA$  and  $N$  phases, whereas **1b** exhibited an  $N$  phase only on cooling. Compound **1c** did not show any LC phases. In the LC phases of **1a**, a fan-shaped texture (Fig. 3a) followed by a schlieren texture (Fig. 3b) were observed on heating, and only a schlieren texture (Fig. 3c) was observed in the LC phase of **1b**. These fan-shaped and schlieren textures are typical for  $SmA$  and  $N$  phases, respectively. Compound **1a** has a very high clearing point (> 300 °C), and it is higher than that of bis-4,4'-(pentafluorobenzoyloxy)biphenyl (**2**<sup>22</sup> in Fig. 2). This result suggests that not only SFA-A but also C-H/F strongly interact between the molecules in the LC phases of **1a**.



- 1a**: X<sub>1</sub> = X<sub>2</sub> = X<sub>3</sub> = F, X<sub>4</sub> = X<sub>5</sub> = H  
**1b**: X<sub>1</sub> = X<sub>2</sub> = F, X<sub>3</sub> = X<sub>4</sub> = X<sub>5</sub> = H  
**1c**: X<sub>1</sub> = F, X<sub>2</sub> = X<sub>3</sub> = X<sub>4</sub> = X<sub>5</sub> = H  
**2**: X<sub>1</sub> = X<sub>2</sub> = X<sub>3</sub> = X<sub>4</sub> = X<sub>5</sub> = F

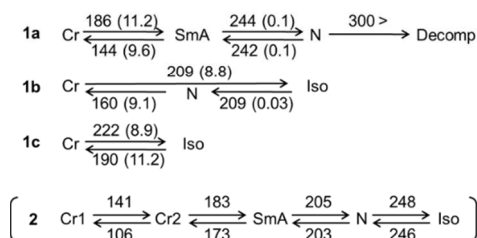


**Fig. 2** Molecular structures and phase transition behaviors of **1a-c**<sup>a)</sup> and **2**.<sup>a,b)</sup>

a) Cr, Cr1, and Cr2 indicate crystal phases.  $SmA$ ,  $N$ , and Iso indicate  $SmA$ ,  $N$ , and isotropic liquid phases, respectively. Decomp indicates decomposition of the compound. The transition temperatures (°C) and transition enthalpies (kcal/mol) were determined by DSC (temperature rate: 5 °C/min) and are given above and below the arrows, respectively. b) The phase transition behavior was reported in reference 22.

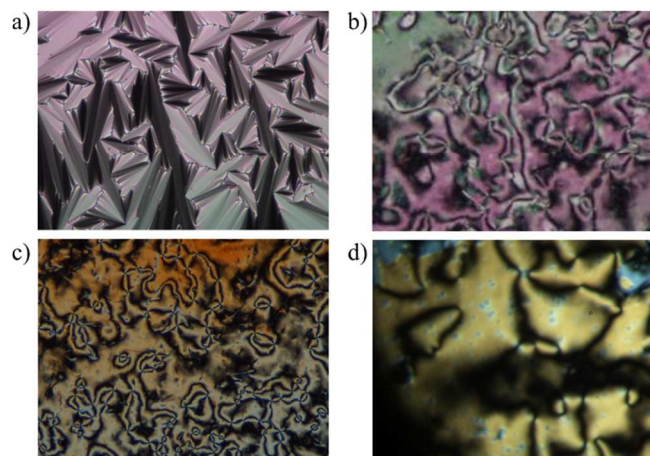


**Fig. 3** Polarized microphotographs ( $\times 200$ , on heating): a) *SmA* phase of **1a** (230 °C), b) *N* phase of **1a** (270 °C), c) *N* phase of **1b** (190 °C), and d) *N* phase of **1a** under an applied magnetic field (255 °C, the direction of magnetic field (3500 gauss) is perpendicular to the glass surface).

The LC sample was sandwiched between two glass plates treated with 1,1,1,3,3,3-hexamethyldisilazane to reduce the hydrophilic interactions between the glass surface and the molecules. Under a magnetic field (3500 gauss), the *N* phase of **1a** exhibited a schlieren textures with all-two-brush disclinations (Fig. 3d), indicative of the possibility of an  $N_b$  phase.<sup>1,32</sup> As shown in Fig. S1, though the *N* phase of **1b** at 190 °C under an applied magnetic field does not show the all-two-brush texture, the texture is very dark and different from that shown in Fig. 3c (190 °C, under no magnetic field).

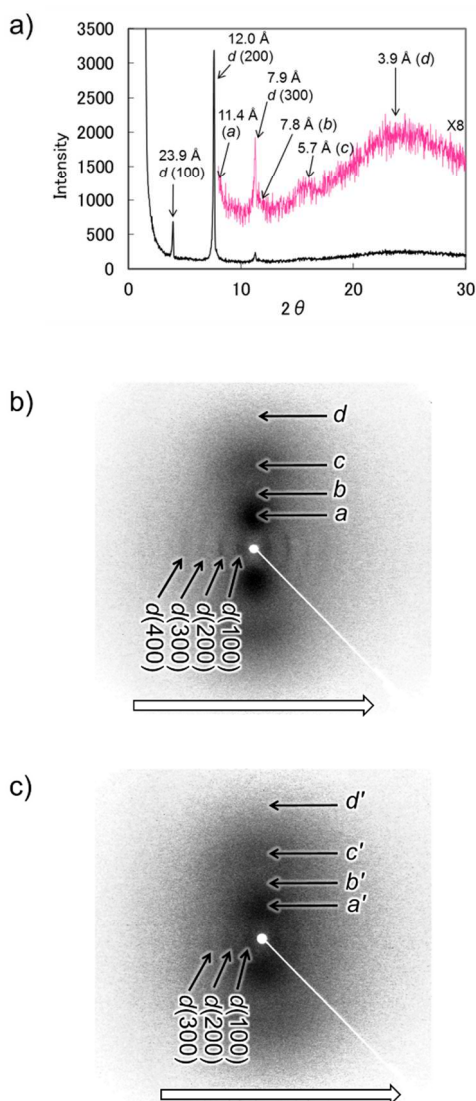


**Fig. 4** a) 1D-XRD profile of **1a** in the *SmA* phase (220 °C) in a reflective method under no magnetic field, b) 2D-XRD profile of **1a** in the *SmA* (220 °C) phase under an applied magnetic field (3500 gauss) and c) 2D-XRD profile of **1a** in the *N* (250 °C) phase under an applied magnetic field (3500 gauss). The interlayer distances ( $d(100)$ ,  $d(200)$  and  $d(300)$ ) and the lateral repeat distances ( $a$ ,  $b$ ,  $c$ ,  $d$ ,  $a'$ ,  $b'$ ,  $c'$  and  $d'$ ) are indicated with black arrows. The direction of the magnetic field is indicated with a large white arrow.

### 1D- and 2D-XRD measurements of **1a** and **1b** in the LC phases

1D- and 2D-XRD profiles of **1a** in the *SmA* and *N* phases are shown in Fig. 4. The sample in LC phase was spread on a glass plate, and the profile was measured in LC phase in a reflective method under no magnetic field. In the 1D-XRD profiles of the *SmA* phase of **1a** shown in Fig. 4a,  $d(100)$ ,  $d(200)$  and  $d(300)$  peaks were observed as sharp peaks at 23.9, 12.0 and 7.9 Å, respectively. This observation indicates that the *SmA* phase has a well-organized layer structure. The molecular length calculated by AM1 method was approximately 25 Å. The intensity of the  $d(200)$  peak is considerably greater than that of the  $d(100)$  peak, which indicates that the main repeat distance in the smectic phase is the half molecular length (12.0 Å) and not the molecular length (23.9 Å). In the magnified XRD profile shown in Fig. 4a, four broad peaks are observed at 11.4 (peak *a*), 7.8 (peak *b*), 5.7 (peak *c*) and 3.9 (peak *d*) Å.

2D-XRD profiles of **1a** packed in a glass capillary (diameter: 1.5 mm) were measured under an applied magnetic field (3500 gauss) in a transmission method. Fig. 4b and 4c present the 2D-XRD profiles of **1a** in the *SmA* (220 °C) and *N* (250 °C) phases. In the *SmA* and *N* phases, the molecular long axes were aligned in parallel to the direction of the magnetic field. In the case of the *SmA* phase (Fig. 4b), the interlayer distances,  $d(100)$ ,  $d(200)$ ,  $d(300)$  and  $d(400)$  are observed in the equator, and the halos *a*, *b*, *c* and *d* are observed on the meridian. The broad peaks *a*, *b*, *c* and *d* correspond to the broad peaks at 11.4, 7.8, 5.7 and 3.9 Å in the 1D-XRD of **1a**, respectively. The 2D-XRD profile of the *N* phase is shown in Fig. 4b. Surprisingly, the *N* phase also has interlayer distances of  $d(100)$ ,  $d(200)$  and  $d(300)$  with the lateral repeat distances ( $a'$ ,  $b'$ ,  $c'$  and  $d'$ ). Accordingly, the *N* phase also has a layered structure and local lateral ordering, although it exhibited the texture of an *N* phase during the POM observations. In the 2D-XRD profile of **1b** in the *N* phase (Fig. S2), the interlayer distances ( $d(200)$  and  $d(300)$ ) were also observed in the equator, but the broad peaks on the meridian were not clear.

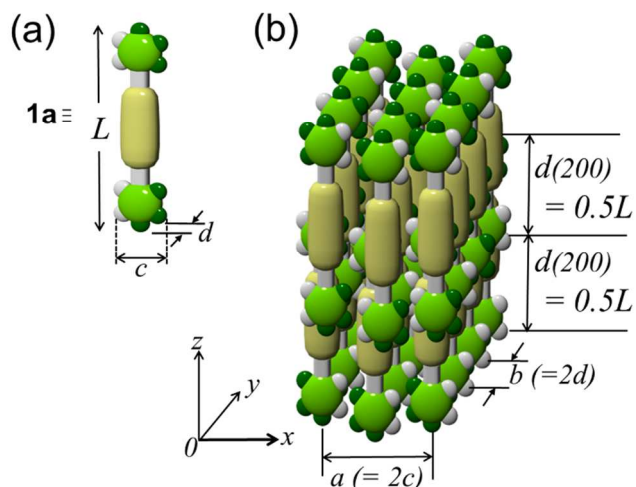


**Fig. 5** Schematic representations of the a) molecular model of **1a** and its sizes ( $L$ : molecular length,  $c$ : molecular width,  $d$ : molecular thickness) (the yellow long

oval disc and the light-green disc containing small dark-green and white spheres indicate a biphenyl moiety and SFP group possessing fluorine and hydrogen atoms, respectively)) and b) estimated molecular packing structure in the *SmA* phase of **1a**, ( $d$ : layer distance ( $\approx 0.5L$ ),  $a$ : twice the molecular width ( $= a(=2c)$  in the  $x$ -axis direction),  $b$ : twice the molecular thickness ( $= b(=2d)$  in the  $y$ -axis direction).

The molecular packing structure of **1a** in the *SmA* phase was postulated from the 1D- and 2D-XRD results, as shown in Fig. 5. In Fig. 5a, the dimensions of molecule **1a** are indicated as  $c \times d \times L$  ( $= \text{width} \times \text{thickness} \times \text{length}$ ). The *SmA* phase of **1a** (Fig. 5b) primarily consists of a layered structure with a half molecular length ( $d \approx 0.5L$ ). In this packing structure, it is estimated that the SFP and biphenyl groups stack with strong intermolecular SFA-A interactions in the  $y$ -axis direction and with intermolecular C-H/F interactions between the two neighboring SFP groups to align the SFP groups in the  $x$ -axis direction. It is assumed that the *N* phase also has a similar layered structure in a short range because of the similarity in the 2D-XRD profiles of the two phases. The packing molecular structure is similar to that of cybotactic *N* phase.<sup>33</sup>

### 2.3 electro-optic measurements of **1a** and **1b** in the LC phases

To investigate their ferroelectric behaviors, electro-optic measurements were conducted. Compound **1a** was sandwiched between two glass plates that were coated with indium-tin-oxide (ITO) and polyimide. The size of the ITO area was 10 mm  $\times$  10 mm, and the cell gap was 5  $\mu\text{m}$ . A triangular wave voltage was applied to the cell while observing the textures of the sample in the cell. The behavior of **1a** in the *SmA* phase was observed using POM at 220  $^{\circ}\text{C}$  (Fig. S3). Before applying the voltage, the sample exhibited a homogeneous texture (Fig. S3a), which indicated that the molecules were aligned parallel to the glass surface. The color of the sample with crossed polarizers was dark green. Upon applying the triangular wave voltage at 0.5-1 Hz, the color of the sample became slightly bright green at approximately  $\pm 50$  V (Fig. S3b) and dark green at approximately 0 V. A change in the brightness was repeatedly observed without a change in the homogeneous texture. Then, the switching behavior in the *N* phase was observed at 270  $^{\circ}\text{C}$  (Fig. S4). Before applying the voltage, the sample exhibited a homogeneous reddish-purple texture as shown in Fig. S4a. Upon applying the voltage at 0.5-1 Hz, the color became light-purple at approximately  $\pm 50$  V (Fig. S4b) and reddish-purple at approximately 0 V. The change in color was repeatedly observed, though the homogeneous texture did not change under applying the triangular wave voltage. It is hypothesized that these results in the *N* and *SmA* phases originate from changes in the directions of the molecular short axes around their molecular long axes.

Switching current response traces obtained in the LC phases of **1a**, **1b** and **2** under a triangular-wave electric field are shown in Fig. 6. As shown in Fig. 6a and 6b, switching current peaks are observed in the *SmA* and *N* phases of **1a**. The peaks (A) in the *SmA* phase are sharper than those (B) in the *N* phase. The *N* phase of **1b** at 200  $^{\circ}\text{C}$  (Fig. 6c) also showed the switching current peaks (C). These switching current peaks indicate that the molecules

change their polar directions cooperatively under an applied triangular wave voltage. Considering the abovementioned POM observation, it indicates that their molecular long axes are maintained parallel to the glass surface and that the molecules are aligned in the rubbing direction of the polyimide film during the entire switching process. Accordingly, the slight changes in the brightness are explained by changes in the birefringence which originate from changes in the alignment of the lateral directions of the molecules via molecular rotation around their molecular long axes.

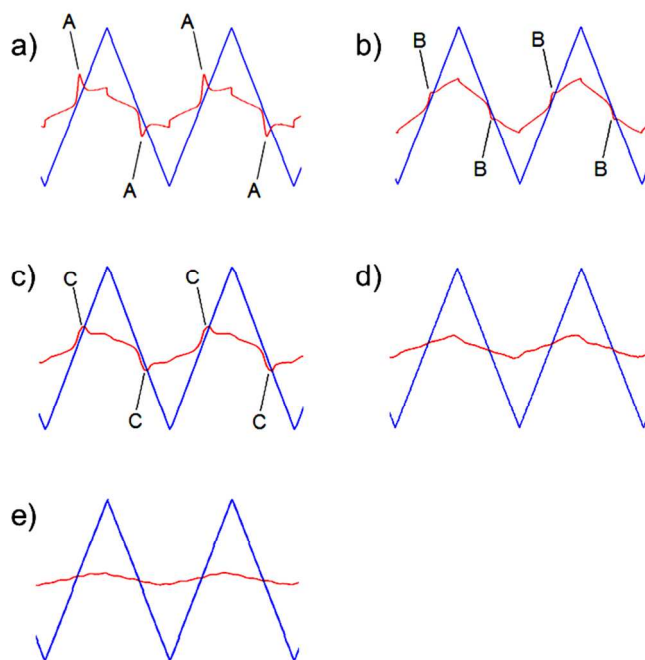


**Fig. 6** Switching current response traces obtained under a triangular-wave electric field; a) **1a** in the *SmA* phase (220  $^{\circ}\text{C}$ , 20 Hz, 100  $V_{pp}$ ), b) **1a** in the *N* phase (270  $^{\circ}\text{C}$ , 20 Hz, 100  $V_{pp}$ ), c) **1b** in the *N* phase (200  $^{\circ}\text{C}$ , 20 Hz, 100  $V_{pp}$ ), d) **2** in the *SmA* phase (190  $^{\circ}\text{C}$ , 20 Hz, 100  $V_{pp}$ ), and e) **2** in the *N* phase (240  $^{\circ}\text{C}$ , 20 Hz, 100  $V_{pp}$ ). The samples were sandwiched between two glass plates coated with a thin ITO layer covered with polyimide (cell gap: 5  $\mu\text{m}$ , ITO area: 10 mm  $\times$  10 mm). The blue and red curves indicate voltage and current. The switching current peaks in (a), (b), and (c) are indicated by A, B, and C, respectively.

To confirm the importance of the SFP groups in **1a**, switching experiment of **2** possessing two pentafluorophenyl groups were performed in the *SmA* and *N* phases under similar conditions. As shown in Fig. 6d and 6e, application of the triangular-wave voltage did not result in switching current peaks in either the *SmA* or *N* phases of **2**. This result clearly indicates that hydrogen atoms at the 5- and 6-positions of the SFP group play an important role in the ferroelectric switching of **1a**.

### 2.4 Estimation of the mechanism for ferroelectric switching in the LC compounds

We estimate the following mechanism for the ferroelectric switching (Fig. 7). The stable conformations were calculated for **1a** by geometry optimization using the density functional

theory (DFT) method, with B3LYP functional and 6-31G(d) basis set.<sup>34</sup> As the result, **1a-anti** and **1a-syn** (Fig. 7a) were obtained as the most stable conformers (Fig. S4). Before applying the voltage, the molecules exist as a mixture of conformers **1a-anti** and **1a-syn** in the *SmA* and *N* phases (Fig. 7b), and the biaxiality of these mesophase is maintained by the face-to-face SFA-A interactions between the SFP group and biphenyl moiety and by the edge-to-edge C-H/F interactions between the neighboring SFP groups.

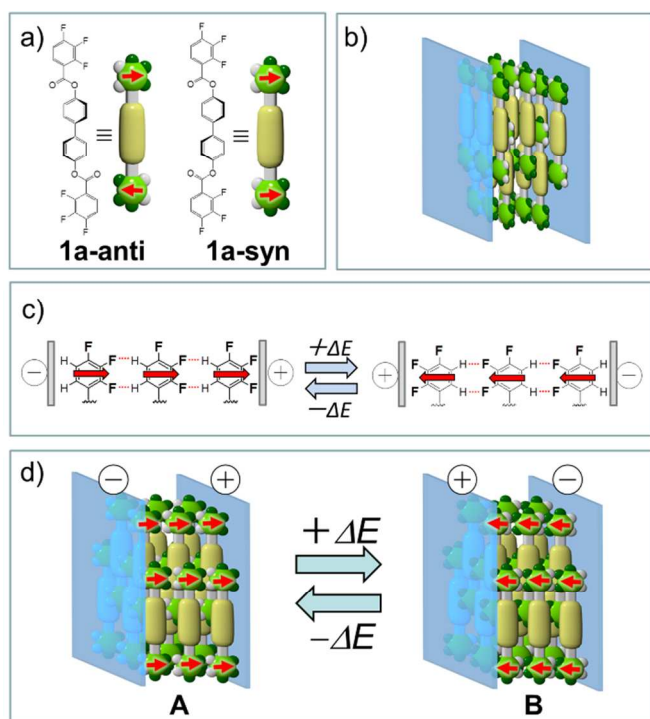


**Fig. 7** Schematic representation of the ferroelectric switching of **1a** in the *SmA* and *N* phases; a) the conformers, **1a-anti** (non-polar) and **1a-syn** (polar), b) a mixture of the conformers at 0 V, c) cooperative switching of the SFP groups (the C-H/F interaction is indicated by a dashed red line) and d) the ferroelectric molecular behaviors under an applied triangular wave voltage (**A** and **B**). The red arrow on the SFP group indicates the polarity of the SFP groups.

As shown in Fig. 7c, under an applied voltage, the SFP groups are uniformly aligned in one direction, and then they change their lateral polar directions under an applied triangular wave voltage. During the switching process the SFP groups rotate around the molecular long axes and change the pairs of CH/F interactions. This cooperative movement of the SFP groups is repeated when applying a triangular wave voltage in the *SmA* and *N* phases. When the voltage is applied, the directions of the C-H/F and SFA-A interactions are parallel and perpendicular to the direction of the electric field, respectively (Fig. 7d, **A** and **B**). The change in the brightness and switching peaks observed in the electro-optic experiments under an applied triangular wave voltage can be explained by the conformational change and/or molecular rotation around the molecular long axis.

## 2.5 Measurement of $P_s$ values of **1a** in the LC phases

Then, the  $P_s$  values in the LC phases of **1a** were investigated as functions of the frequency, voltage, and temperature (Fig. 8). In Fig. 8a, the  $P_s$  value in the *SmA* phase (200 °C) was plotted against the frequency (applied voltage: 50  $V_{pp}$ ). The  $P_s$  values are slightly decrease or mostly in a range of  $40 \pm 10$  nC/cm<sup>2</sup> from 10 to 100 Hz. The almost constant responsiveness of **1a** against the frequency originates in the small excluded volume during the switching process. This also indicates that the switching peaks do not originate from movement of ionic impurity because ionic impurity in LC phases cannot move at more than 10 Hz.<sup>35,36</sup> As shown in Fig. 8b, the  $P_s$  value saturates at more than 160  $V_{pp}$ . As shown in Fig. 8c the  $P_s$  is the largest at approximately 230 °C in the *SmA* phase. However, in the *N* phase the  $P_s$  value decreases as the temperature increases, which indicates that the molecular movements in the *N* phase are not restricted in comparison with those in the *SmA* phase. It is assumed that the lateral polar directions of the molecules cannot be controlled by the applied voltage in the higher temperature range in the *N* phase.

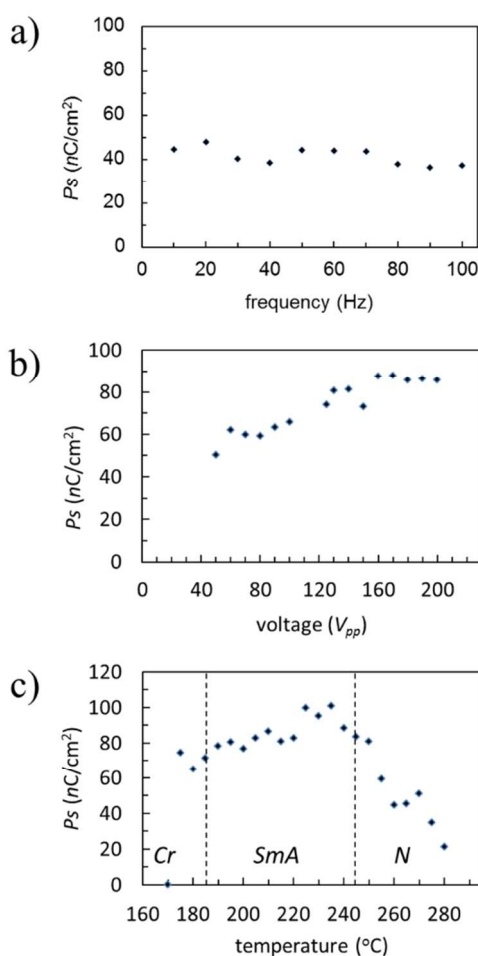


**Fig. 8** Plot of the  $P_s$  values of **1a**; a) against the frequency (Hz) in the *SmA* phase ( $T = 200$  °C) (Voltage = 50  $V_{pp}$ , cell area = 1 cm $\times$ 1 cm, cell gap = 5  $\mu$ m), b) against the applied voltage in the *SmA* phase ( $T = 200$  °C) (Frequency = 20 Hz, cell area = 1 cm $\times$ 1 cm, cell gap = 5  $\mu$ m) and c) against the temperature (Voltage = 150  $V_{pp}$ ,

frequency = 20 Hz, cell area = 1 cm $\times$ 1 cm, cell gap = 5  $\mu$ m.) The dashed lines indicate the crystal-*SmA* (186 °C) and *SmA-N* (244 °C) phase transition temperatures, respectively.

## Conclusion

We realized the locally biaxial *N* and *SmA* phases of **1a** and **1b** and confirmed their ferroelectric switching. It is believed that our methodology for realizing local biaxiality through introducing intermolecular SFA-A and C-H/F interactions and its utilization for ferroelectric LC phases, are useful for designing novel ferroelectric LC materials. Although it is currently thought that these ferroelectrically switchable *N<sub>b</sub>* or *SmA<sub>b</sub>* phases are not suitable for light-switching devices because of the low birefringence in the direction perpendicular to the molecular long axis, our rod-like molecules have a large advantage in the high responsiveness under an applied electric field. In this study, we call our molecules as “rod-like”. However, from these results, it may be that they should be called “board-shaped” with *C<sub>2</sub>* symmetry than “rod-like” which assumes the *D $\infty$*  symmetry. We believe that this new concept for ferroelectric *N<sub>b</sub>* and *SmA<sub>b</sub>* phases using straight rod molecules will have a strong impact on the field of LC science.

## Experimental

**X-ray diffraction.** The one-dimensional X-ray diffraction (1D-XRD) measurements on thin layered samples on glass (0.15 mm thickness) were carried out by a Rigaku RINT-2000 diffractometer (Cu-target X-ray tube, 40 kV, 30 mA). The two-dimensional X-ray diffraction (2D-XRD) measurements on film samples (1 mm thickness) suspended in a hole (1 mm diameter) of an aluminium plate (2 mm thickness) were carried out by a TRY-SE TRY-DXGSA-HHIP diffractometer (Cu-target X-ray tube, 40 kV, 30 mA). The X-ray beam (0.5 mm diameter) was vertically irradiated to the suspended sample film from its upper side, and the X-ray scattering patterns were recorded on an imaging plate and developed by a FUJIFILM FLA-7000 imaging reader. Samarium-cobalt magnets were used for alignment of LC compounds.

**Optoelectronic experiment:** The LC samples were put in a transparent sandwich-type capacitor cell consisting of two ITO coated glass plates (ITO area size: 10 mm $\times$ 10 mm, cell gap: 5 $\mu$ m) whose glass surfaces were coated with a polyimide thin film and the two thin films were rubbed in anti-parallel. A Nikon ECLIPSE E400POL microscope equipped with a hot stage system STC200D (Instec, Inc.) was used for observation of textures of LC samples. The triangular wave voltage generated by a Yokogawa FG110 synthesized function generator and an FLC Electronics voltage amplifier F10A was applied to the samples. The current in response to an applied triangular-wave field was measured by a KEYENCE NR-2000 data acquisition system.

**Synthesis of compound 1a:** 4,4'-Biphenol (0.0530 g, 0.285 mmol), 2,3,4-trifluorobenzoic acid (0.101 g, 0.574 mmol), and THF (10 mL) were placed in a 200 mL round-bottom flask. The mixture was cooled at 0 °C. To the mixture were added 4-(*N,N*-dimethylamino)pyridine (0.020 g, 0.16 mmol) and *N,N'*-diisopropylcarbodiimide (0.110 mL, 0.715 mmol), and then the mixture was warmed to room temperature and stirred for 48 h. The organic phase was washed with water (100 mL) and saturated aqueous NaHCO<sub>3</sub> solution (50 mL) and dried over anhydrous sodium sulfate. The solvent was removed by evaporation. The crude product was purified by silica gel column chromatography eluting with chloroform. The crude

product was recrystallized from chloroform/hexane. Compounds **1b** and **1c** are also prepared with the same procedure.

**1a:** 25%; white solid; Rf. 0.51 (chloroform); IR (KBr):  $\nu$  = 3050, 1731 (C=O), 1477, 1320, 1300, 1213, 1047, 863 cm<sup>-1</sup>; <sup>1</sup>H NMR (300 MHz, CDCl<sub>3</sub>, 20 °C, TMS):  $\delta$  = 7.14 (m, 2 H), 7.32 (dt, *J* = 8.7 and 1.9 Hz, 4 H), 7.65 (dt, *J* = 8.7 and 2.3 Hz, 4 H), 7.94 (m, 2H); <sup>13</sup>C NMR (75 MHz, CDCl<sub>3</sub>, 20 °C, TMS):  $\delta$  = 112.9, 119.1, 122.3, 127.7, 128.4, 134.5, 138.9, 162.2 (The carbon atoms bearing a fluorine atom could not be observed); HRMS (APCI) calcd for C<sub>26</sub>H<sub>12</sub>O<sub>4</sub>F<sub>6</sub> [M<sup>+</sup>], 502.0634; found, 502.0625.

**1b:** 15%; white solid; Rf. 0.69 (chloroform); IR (KBr):  $\nu$  = 3097, 1730 (C=O), 1485, 1291, 1199, 750 cm<sup>-1</sup>; <sup>1</sup>H NMR (300 MHz, CDCl<sub>3</sub>, 20 °C, TMS):  $\delta$  = 7.25 (m, 2 H), 7.32 (d, *J* = 8.7 Hz, 4 H), 7.45 (m, 2 H), 7.64 (d, *J* = 8.7 Hz, 4 H), 7.89 (m, 2 H); <sup>13</sup>C NMR (75 MHz, CDCl<sub>3</sub>, 20 °C, TMS):  $\delta$  = 122.3, 122.7, 124.4, 127.5, 128.7, 138.9, 150.4, 162.4 (The carbon atoms bearing a fluorine atom could not be observed); HRMS (APCI) calcd for C<sub>26</sub>H<sub>15</sub>O<sub>4</sub>F<sub>4</sub> [M<sup>+</sup>+H], 467.0901; found, 467.0890.

**1c:** 50%; white solid; Rf. 0.65 (chloroform); IR (KBr):  $\nu$  = 2960, 1742 (C=O), 1489, 1197, 1054, 763 cm<sup>-1</sup>; <sup>1</sup>H NMR (300 MHz, CDCl<sub>3</sub>, 20 °C, TMS):  $\delta$  = 7.30 (m, 4 H), 7.34 (m, 4 H), 7.63 (m, 4 H), 7.63 (m, 2 H), 8.14 (td, *J* = 8.3 and 1.5 Hz, 2 H); <sup>13</sup>C NMR (75 MHz, CDCl<sub>3</sub>, 20 °C, TMS):  $\delta$  = 117.5, 117.8, 122.4, 128.64, 133.0, 135.6, 135.7, 138.7, 150.5, 161.0, 163.2; HRMS (APCI) calcd for C<sub>26</sub>H<sub>17</sub>O<sub>4</sub>F<sub>2</sub> [M<sup>+</sup>+H], 431.1089; found, 431.1078.

## Acknowledgements

We thank Dr. H. Ozaki who saved KK's life by an operation for brain haemorrhage during the term of this project. This work was supported by Japan Society for the Promotion of Science KAKENHI Grant Numbers 24655166, 25288088.

## Notes and References

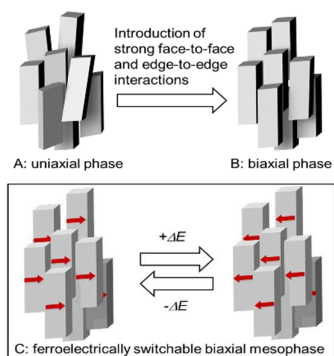
Department of Applied Chemistry and Biotechnology, Faculty of Engineering, Chiba University, 1-33 Yayoi-cho, Inage-ku, Chiba 263-8522, Japan. E-mail: kishikawa@faculty.chiba-u.jp

† Electronic Supplementary Information (ESI) available: [Fig. S1 (microphotograph of the *N* phase of **1b** at 190 °C under an applied magnetic field), Fig. S2 (2D-XRD profile of **1b** in the *N* phase at 200°C under applying a magnetic field), Fig. S3 (microphotographs of **1a** in the *SmA* phase (220 °C) at 0 V and +50V), Fig. S4 (microphotographs of **1a** in the *N* phase (270 °C) at 0 V and +50V), and Fig. S5 (four stable conformers of **1a** obtained by DFT calculation)]. See DOI: 10.1039/b000000x/

- 1 C. Tschierske and D. J. Photinos, *J. Mater. Chem.*, 2010, **20**, 4263.
- 2 M. Lehmann, *Liq. Cryst.*, 2011, **38**, 1389.
- 3 (a) Y. Shimbo, E. Gorecka, D. Pochiecha, F. Araoka, M. Goto, Y. Takanishi, K. Ishikawa, J. Mieczkowski, K. Gomola and H. Takezoe, *Phys. Rev. Lett.*, 2006, **97**, 113901; (b) Y. Shimbo, Y. Takanishi, K. Ishikawa, E. Gorecka, D. Pochiecha, J. Mieczkowski, K. Gomola and H. Takezoe, *Jpn. J. Appl. Phys.*, 2006, **45**, L282.
- 4 (a) G. R. Luckhurst, *Thin Solid Films*, 2001, **393**, 40; (b) J.-H. Lee, T.-K. Lim, W.-T. Kim and J.-I. Jin, *J. Appl. Phys.*, 2007, **101**, 034105.
- 5 M. W. Schröder, S. Diele, N. Pancenko, W. Weissflog and G. Pelzl, *J. Mater. Chem.*, 2002, **12**, 1331.
- 6 C. V. Yelamaggad, I. S. Shashikala, D. S. S. Rao, G. G. Nair and S. K. Prasad, *J. Mater. Chem.*, 2006, **16**, 4099.

- 7 (a) B. K. Sadashiva, R. A. Reddy, R. Pratibha and N. V. Madhusudana, *Chem. Commun.*, 2001, 2140; (b) B. K. Sadashiva, R. A. Reddy, R. Pratibha and N. V. Madhusudana, *J. Mater. Chem.*, 2002, **12**, 943.
- 8 C. Köhn, J. Figueirinhas, G. Feio, C. Cruz and R. Y. Dong, *Chem. Eur. J.*, 2010, **16**, 8275.
- 9 (a) L. A. Madsen, T. J. Dingemans, M. Nakata and E. T. Samulski, *Phys. Rev. Lett.*, 2004, **92**, 145505; (b) E. T. Samulski, *Liq. Cryst.*, 2010, **37**, 669; (c) F. Speetjens, J. Lindborg, T. Tauscher, N. LaFemina, J. Nguyen, E. T. Samulski, F. Vita, O. Francescangeli and E. Scharer, *J. Mater. Chem.*, 2012, **22**, 22558; (d) T. J. Dingemans, L. A. Madsen, O. Francescangeli, F. Vita, D. J. Photinos, C.-D. Poon and E. T. Samulski, *Liq. Cryst.*, 2013, **40**, 1655.
- 10 Y.-K. Kim, M. Majumdar, B. I. Senyuk, L. Tortora, J. Selmann, M. Lehmann, A. Jäkl, J. T. Gleeson, O. D. Lavrentovich and S. Sprunt, *Soft Matter*, 2012, **8**, 8880.
- 11 K. Geese, M. Prehm and C. Tschierske, *Chem. Commun.*, 2014, **50**, 9903.
- 12 (a) T. Hegmann, J. Kain, S. Diele, G. Pelzl and C. Tschierske, *Angew. Chem. Int. Ed. Engl.*, 2001, **40**, 887; (b) L. Omnès, B. A. Timimi, T. Gelbrich, M. B. Hursthouse, G. R. Luckhurst and D. W. Bruce, *Chem. Commun.*, 2001, 2248; (c) A. G. Vanakaras, M. A. Bates and D. J. Photinos, *Phys. Chem. Chem. Phys.*, 2003, **5**, 3700; (d) K. Kaznacheev and T. Hegmann, *Phys. Chem. Chem. Phys.*, 2007, **9**, 1705.
- 13 (a) J. J. Hunt, R. W. Date, B. A. Timimi, G. R. Luckhurst and D. W. Bruce, *J. Am. Chem. Soc.*, 2001, **123**, 10115; (b) D. Apreutesei and G. H. Mehl, *Chem. Commun.*, 2006, 609; (c) K.-U. Jeong, A. J. Jing, B. Mansdorf, M. J. Graham, D.-K. Yang, F. W. Harris and S. Z. D. Cheng, *Chem. Mater.*, 2007, **19**, 2921.
- 14 C. V. Yelamaggad, I. S. Shashikala, V. P. Tamilenth, D. S. S. Rao, G. G. Nair and S. K. Prasad, *J. Mater. Chem.*, 2008, **18**, 2096.
- 15 C. V. Yelamaggad, V. P. Tamilenth, D. S. S. Rao, G. G. Nair and S. K. Prasad, *J. Mater. Chem.*, 2009, **19**, 2906.
- 16 (a) C. V. Yelamaggad, S. K. Prasad, G. G. Nair, I. Shashikala, D. S. S. Rao, C. V. Lobo and S. Chandrasekhar, *Angew. Chem. Int. Ed. Engl.*, 2004, **43**, 3429; (b) Y. Wang, H. G. Yoon, H. K. Bisoyi, S. Kumar and Q. Li, *J. Mater. Chem.*, 2012, **22**, 20363.
- 17 (a) H. F. Leube and H. Finkelmann, *Makromol. Chem.*, 1991, **192**, 1317; (b) R. Storz, A. Komp, A. Hoffmann and H. Finkelmann, *Macromol. Rapid Commun.*, 2009, **30**, 615; (c) F. Brömmel, P. Zou, H. Finkelmann and A. Hoffmann, *Soft Matter*, 2013, **9**, 1674.
- 18 (a) R. Prathiba, N. V. Madhusudana and B. K. Sadashiva, *Science*, 2000, **288**, 2184; (b) I. I. Smalyukh, R. Pratibha, N. V. Madhusudana and O. D. Lavrentovich, *Eur. Phys. J. E*, 2005, **16**, 179.
- 19 O. Francescangeli, V. Stanic, S. I. Torgova, A. Strigazzi, N. Scaramuzza, C. Ferrero, I. P. Dolbnya, T. M. Weiss, R. Berardi, L. Muccioli, S. Orlandi and C. Zannoni, *Adv. Funct. Mater.*, 2009, **19**, 2592.
- 20 G. Shanker, M. Nagaraj, A. Kocot, J. K. Vij, M. Prehm and C. Tschierske, *Adv. Funct. Mater.*, 2012, **22**, 1671.
- 21 R. Berardi and C. Zannoni, *J. Chem. Phys.*, 2000, **113**, 5971.
- 22 K. Kishikawa, S. Aikyo, S. Akiyama, T. Inoue, M. Takahashi, S. Yagai, H. Aonuma and S. Kohmoto, *Soft Matter*, 2011, **7**, 5176.
- 23 K. Kishikawa, T. Inoue, Y. Sasaki, S. Aikyo, M. Takahashi and S. Kohmoto, *Soft Matter*, 2011, **7**, 7532.
- 24 (a) C. R. Patrick and G. S. Prosser, *Nature*, 1960, **187**, 1021; (b) J. H. Williams, *Acc. Chem. Res.*, 1993, **26**, 593; (c) E. A. Meyer, R. K. Castellano and F. Diederich, *Angew. Chem. Int. Ed. Engl.*, 2003, **42**, 1210.
- 25 (a) G. W. Coates, A. R. Dunn, L. M. Henling, D. A. Dougherty and R. H. Grubbs, *Angew. Chem. Int. Ed. Engl.*, 1997, **36**, 248; (b) G. W. Coates, A. R. Dunn, L. M. Henling, J. W. Ziller and R. H. Grubbs, *J. Am. Chem. Soc.*, 1998, **120**, 3641; (c) H. Lee, C. B. Knobler and M. F. Hawthorne, *Chem. Commun.*, 2000, 2485.
- 26 K. Kishikawa, K. Oda, S. Aikyo and S. Kohmoto, *Angew. Chem. Int. Ed. Engl.*, 2007, **46**, 764.
- 27 (a) H.-C. Weiss, R. Boese, H. L. Smith and M. M. Haley, *Chem. Commun.*, 1997, 2403; (b) V. R. Thalladi, H.-C. Weiss, D. Bläser, R. Boese, A. Nangia and G. R. Desiraju, *J. Am. Chem. Soc.*, 1998, **120**, 8702; (c) S. Tsuzuki, T. Uchimaru, M. Mikami and S. Urata, *J. Phys. Chem. A*, 2003, **107**, 7962; (d) W. Caminati, J. C. Lopez, J. L. Alonso and J.-U. Grabow, *Angew. Chem. Int. Ed. Engl.*, 2005, **44**, 3840; (e) M. Horiguchi, S. Okuhara, E. Shimano, D. Fujimoto, H. Takahashi, H. Tsue and R. Tamura, *Cryst. Growth Des.*, 2008, **8**, 540.
- 28 (a) S. Lorenzo, G. R. Lewis and I. Dance, *New. J. Chem.*, 2000, **24**, 295; (b) O. R. Lozman and R. J. Bushby, J. G. Vinter, *J. Chem. Soc. Perkin Trans.*, 2, 2001, 1446.
- 29 (a) J. H. Williams, J. K. Cockcroft and A. N. Fitch, *Angew. Chem. Int. Ed. Engl.*, 1992, **31**, 1655; (b) V. E. Williams, R. P. Lemieux and G. R. J. Thatcher, *J. Org. Chem.*, 1996, **61**, 1927; (c) J. Hernandez-Trujillo, F. Colmenares, G. Cuevas and M. Costas, *Chem. Phys. Lett.*, 1997, **265**, 503; (d) A. P. West, Jr., S. Mecozzi and D. A. Dougherty, *J. Phys. Org. Chem.*, 1997, **10**, 347; (e) C. B. Martin, H. R. Mulla, P. G. Willis and A. Cammers-Goodwin, *J. Org. Chem.*, 1999, **64**, 7802.
- 30 F. Cozzi, F. Ponzini, R. Annunziata, M. Cinquini and J. S. Siegel, *Angew. Chem. Int. Ed. Engl.*, 1995, **34**, 1019.
- 31 (a) E. Kryachko and S. Scheiner, *J. Phys. Chem. A*, 2004, **108**, 2527; (b) E. D'Oría and J. J. Novoa, *CrystEngComm*, 2008, **10**, 423.
- 32 (a) S. Chandrasekhar, R. B. Ratna, B. K. Sadashiva and V. N. Raja, *Mol. Cryst. Liq. Cryst.*, 1988, **165**, 123; (b) S. Chandrasekhar, G. G. Nair, D. S. S. Rao, S. K. Prasad, K. Praefcke and D. Singer, *Mol. Cryst. Liq. Cryst.*, 1996, **288**, 7; (c) Y. Galerne, *Mol. Cryst. Liq. Cryst.*, 1998, **323**, 211; (d) M. Lehmann, S.-W. Kang, C. Köhn, S. Haseloh, U. Kolb, D. Schollmeyer, Q. B. Wang and S. Kumar, *J. Mater. Chem.*, 2006, **16**, 4326; (e) B. R. Acharya, S.-W. Kang, V. Prasad and S. Kumar, *J. Phys. Chem. B*, 2009, **113**, 3845.
- 33 (a) C. Keith, A. Lehmann, U. Baumeister, M. Prehm and C. Tschierske, *Soft Matter*, 2010, **6**, 1704; (b) O. Francescangeli and E. T. Samulski, *Soft Matter*, 2010, **6**, 2413; (c) H.-H. Chen, H.-A. Lin, Y.-H. Lai, S.-Y. Lin, C.-H. Chiang, H.-F. Hsu, T.-L. Shih, J.-J. Lee, C.-C. Lai and T.-S. Kuo, *Chem. Eur. J.* 2012, **18**, 9543.
- 34 Gaussian 09, Revision D.01, M. J. Frisch, G. W. Trucks, H. B. Schlegel, G. E. Scuseria, M. A. Robb, J. R. Cheeseman, G. Scalmani, V. Barone, B. Mennucci, G. A. Petersson, H. Nakatsuji, M. Caricato, X. Li, H. P. Hratchian, A. F. Izmaylov, J. Bloino, G. Zheng, J. L. Sonnenberg, M. Hada, M. Ehara, K. Toyota, R. Fukuda, J. Hasegawa, M. Ishida, T. Nakajima, Y. Honda, O. Kitao, H. Nakai, T. Vreven, J. A. Montgomery, Jr., J. E. Peralta, F. Ogliaro, M. Bearpark, J. J. Heyd, E. Brothers, K. N. Kudin, V. N. Staroverov, R. Kobayashi, J. Normand, K. Raghavachari, A. Rendell, J. C. Burant, S. S. Iyengar, J. Tomasi, M. Cossi, N. Rega, J. M. Millam, M. Klene, J. E. Knox, J. B. Cross, V. Bakken, C. Adamo, J. Jaramillo, R. Gomperts, R. E. Stratmann, O. Yazyev, A. J. Austin, R. Cammi, C. Pomelli, J. W. Ochterski, R. L. Martin, K. Morokuma, V. G. Zakrzewski, G. A. Voth, P. Salvador, J. J. Dannenberg, S. Dapprich, A. D. Daniels, Ö. Farkas, J. B. Foresman, J. V. Ortiz, J. Cioslowski and D. J. Fox, Gaussian, Inc., Wallingford CT, 2009.
- 35 (a) D. Kilian, D. Knawby, M. A. Athanassopoulou, S. T. Trzaska, T. M. Swager, S. Wróbel and W. Haase, *Liq. Cryst.*, 2000, **27**, 509; (b) W. Haase, D. Kilian, M. A. Athanassopoulou, D. Knawby, T. M. Swager and S. Wróbel, *Liq. Cryst.*, 2002, **29**, 133.
- 36 K. Kishikawa, S. Nakahara, Y. Nishikawa, S. Kohmoto and M. Yamamoto, *J. Am. Chem. Soc.*, 2005, **127**, 2565.

## Table of contents entry



Local biaxiality was realized through perfluoroarene-arene and CH/F interactions in the smectic A and nematic phases of rod-like compound **1a**, and a ferroelectric switching was observed.